4th Symposium of Turkish Society for Photogrammetry and Remote Sensing, Istanbul, Turkey, June 5-7, 2007.
http://www.photogrammetry.ethz.ch/general/persons/devrim_publ.html

LEAST SQUARES MATCHING OF 3D SURFACES

Devrim Akca

Institute of Geodesy and Photogrammetry, ETH Zurich, CH 8093 Zurich, Switzerland – akca@geod.baug.ethz.ch
www.photogrammetry.ethz.ch

Commission V, WG V/3

KEYWORDS: Least Squares matching, surface matching, pointcloud, laser scanning

ABSTRACT:

An algorithm for the least squares matching of overlapping 3D surfaces is presented. It estimates the transformation parameters of one or more fully 3D surfaces with respect to a template one, using the Generalized Gauss-Markoff model, minimizing the sum of squares of the Euclidean distances between the surfaces. This formulation gives the opportunity of matching arbitrarily oriented 3D surfaces simultaneously, without using explicit tie points. Besides the mathematical model of the procedure, we discuss the computational aspects. We give practical examples to demonstrate the method.

1. INTRODUCTION

In the literature, several attempts have been described concerning the registration of 3D pointclouds. One of the most popular methods is the Iterative Closest Point (ICP) algorithm developed by Besl and McKay (1992), Chen and Medioni (1992) and Zhang (1994). The ICP is based on the search for pairs of nearest points in two data sets and estimates the rigid body transformation that aligns them. Then, the rigid body transformation is applied to the points of one set and the procedure is iterated until convergence is achieved.

In Besl and McKay (1992) and Zhang (1994) the ICP requires every point in one surface to have a corresponding point on the other surface. Alternatively, the distance between the transformed points in one surface and the corresponding tangent planes on the other surface was used as a registration evaluation function (Chen and Medioni, 1992; Bergevin et al., 1996; Pulli, 1999). The point-to-tangent plane approach gives a better registration accuracy than the point-to-point approach. It was originally proposed by Potmesil (1983).

The outliers due to erroneous measurements (e.g. points on the object silhouette) and occlusions may significantly impair the quality of the registration. The following strategies have been proposed for localization and elimination of outliers and occlusions: rejection of pairs based on predefined (constant) distance threshold (Turk and Levoy, 1994; Zhang, 1994; Blais and Levine, 1995; Guehring, 2001; Dalley and Flynn, 2002) or variable distance thresholds adapted from Robust Estimation Methods (Masuda and Yokoya, 1995; Neugebauer, 1997; Fitzgibbon, 2001; Gruen and Akca, 2005), rejection of pairs based on the orientation threshold for surface normals (Zhang, 1994; Guehring, 2001), rejection of pairs containing points on mesh boundaries (Turk and Levoy, 1994; Pulli, 1999; Guehring, 2001), rejection of pairs based on the reciprocal correspondence (Pajdla and Van Gool, 1995), rejection of the worst n% of pairs (Pulli, 1999), employing the least median of squares (LMS or LMedS) (Masuda and Yokoya, 1995) and the least trimmed squares estimators (Chetverikov et al., 2005).

In the ICP algorithm and its variants, main emphasis is put on the estimation of a 6-parameter rigid body transformation without uniform scale factor. There are a few reports in which higher order geometric transformations are formulated (Feldmar and Ayache, 1996; Szeliski and Lavallee, 1996).

The parameters of the rigid body transformation are generally estimated by the use of closed-form solutions, mainly singular value decomposition (SVD) (Arun et al., 1987; Horn et al., 1988) and quaternion methods (Faugeras and Hebert, 1986; Horn, 1987). Eggert et al. (1997) and Williams et al. (1999) provide an extensive review and comparison. The closed-form solutions can only estimate the parameters of a rigid body or a similarity transformation.

The closed-form solutions cannot fully consider the statistical point error models. Zhang (1994) and Dorai et al. (1997) weighted the individual points based on a priori noise information. Williams et al. (1999), Guehring (2001) and Okatani and Deguchi (2002) proposed methods that can model the anisotropic point errors.

The gradient descent type of algorithms can support full stochastic models for measurement errors, and assure a substantially lower number of iterations than the ICP variants (Szeliski and Lavallee, 1996; Neugebauer, 1997; Fitzgibbon, 2001). The Levenberg-Marquardt method is usually adopted for the estimation.

The ICP, and in general all surface registration methods, require heavy computations. Strategies, mainly employed to reduce the computation time are: reduction of the number of iterations, reduction of the number of employed points, and speeding up the correspondence computation. Extensive surveys on commonly used methods are given in Akca and Gruen (2005b), Jost and Huegli (2003) and Park and Subbarao (2003).

Several reviews and comparison studies on surface registration methods are available in the literature (Jokinen and Haggren, 1998; Williams et al., 1999; Campbell and Flynn, 2001; Rusinkiewicz and Levoy, 2001; Gruen and Akca, 2005).

In Photogrammetry, the problem statement of surface patch matching and its solution method was first addressed by Gruen (1985) as a straight extension of Least Squares matching (LSM).

There have been some studies on the absolute orientation of stereo models using Digital Elevation Models (DEM) as control information (Ebner and Strunz, 1988; Rosenholm and Torlegard, 1988). This work is known as DEM matching. This method basically estimates the 3D similarity transformation parameters between two DEM patches, minimizing the sum of squares of differences along the *z*-axes. Schenk et al. (2000) showed the clear advantage of minimization of distances along surface normals against to minimization of elevation differences. Beside the many other applications it has been used for the registration of airborne laser scanner strips as well (Maas, 2000; Postolov et al., 1999). The DEM matching corresponds mathematically to Least Squares image matching, but can only be applied to 2.5D surfaces, which is of limited value in case of generally formed objects.

In our previous work an algorithm for Least Squares matching of overlapping 3D surfaces was given (Gruen and Akca, 2005). It estimates the transformation parameters of one or more fully 3D surfaces with respect to a template one, using the Generalized Gauss-Markoff model, minimizing the sum of squares of the Euclidean distances between the surfaces. This formulation gives the opportunity of matching arbitrarily oriented 3D surfaces simultaneously, without using explicit tie points. Our mathematical model is a generalization of the Least Squares image matching method, in particular the method given by Gruen (1985). We gave further extensions of the basic model: simultaneous matching of multi sub-surface patches, and matching of surface geometry and its attribute information, e.g. reflectance, color, temperature, etc. under a combined estimation model (Akca and Gruen, 2005a).

In this study we focus on the computational aspects with regard to outlier and occlusion detection and the optimization of the run-time of the correspondence computation. The details of the mathematical modeling of the proposed method and the execution aspects are explained in the following section. The two strategies for the fast correspondence computation are given in the third section. Practical examples to demonstrate the feasibility of the method are presented in the fourth section.

2. LEAST SQUARES 3D SURFACE MATCHING

2.1 The basic estimation model

Assume that two partial surfaces of an object were digitized at different times or from different viewpoints or by different sensors. $f(x, y, z)$ and $g(x, y, z)$ are conjugate regions of the object in the template and search surfaces, respectively. Both of them are discrete 3D approximations of the continuous function of the object surface. The surface representation can be carried out in any piecewise form. $f(x, y, z)$ and $g(x, y, z)$ stand for any surface element of this representation.

The problem is estimating the parameters of a 3D transformation, which satisfies the Least Squares matching of the search surface $g(x, y, z)$ to the template $f(x, y, z)$. In an ideal situation one would have

$$f(x,y,z) = g(x,y,z) \tag{1}$$

Because of the effects of random errors, Equation (1) is not consistent. Therefore, a true error vector $e(x, y, z)$ is added, assuming that the template noise is independent of the search noise.

$$f(x,y,z) - e(x,y,z) = g(x,y,z) \tag{2}$$

Equation (2) are observation equations, which functionally relate the observations $f(x, y, z)$ to the parameters of $g(x, y, z)$. The matching is achieved by Least Squares minimization of a goal function, which measures the sum of the squares of the Euclidean distances between the surfaces. The final location is estimated with respect to an initial position of $g(x, y, z)$, the approximation of the conjugate search surface $g^0(x, y, z)$.

To express the geometric relationship between the conjugate surface patches, a 7-parameter 3D similarity transformation is used:

$$\begin{aligned} x &= t_x + m(r_{11}x_0 + r_{12}y_0 + r_{13}z_0) \\ y &= t_y + m(r_{21}x_0 + r_{22}y_0 + r_{23}z_0) \\ z &= t_z + m(r_{31}x_0 + r_{32}y_0 + r_{33}z_0) \end{aligned} \tag{3}$$

where $r_{ij} = \mathbf{R}(\omega,\varphi,\kappa)$ is the orthogonal rotation matrix, $[t_x\ t_y\ t_z]^T$ is the translation vector, and m is the uniform scale factor. This parameter space can be extended or reduced, as the situation demands it.

In order to perform a Least Squares estimation, Equation (2) is expanded using the Taylor series, of which only the linear terms are retained:

$$\begin{aligned} f(x,y,z) - e(x,y,z) = g^0(x,y,z) &+ \frac{\partial g^0(x,y,z)}{\partial x}\mathrm{d}x \\ &+ \frac{\partial g^0(x,y,z)}{\partial y}\mathrm{d}y + \frac{\partial g^0(x,y,z)}{\partial z}\mathrm{d}z \end{aligned} \tag{4}$$

with

$$\mathrm{d}x = \frac{\partial x}{\partial p_i}\mathrm{d}p_i \quad , \quad \mathrm{d}y = \frac{\partial y}{\partial p_i}\mathrm{d}p_i \quad , \quad \mathrm{d}z = \frac{\partial z}{\partial p_i}\mathrm{d}p_i \tag{5}$$

where $p_i \in \{t_x, t_y, t_z, m, \omega, \varphi, \kappa\}$ is the i-th transformation parameter in Equation (3). Differentiation of Equation (3) gives:

$$\begin{aligned} \mathrm{d}x &= \mathrm{d}t_x + a_{10}\,\mathrm{d}m + a_{11}\,\mathrm{d}\omega + a_{12}\,\mathrm{d}\varphi + a_{13}\,\mathrm{d}\kappa \\ \mathrm{d}y &= \mathrm{d}t_y + a_{20}\,\mathrm{d}m + a_{21}\,\mathrm{d}\omega + a_{22}\,\mathrm{d}\varphi + a_{23}\,\mathrm{d}\kappa \\ \mathrm{d}z &= \mathrm{d}t_z + a_{30}\,\mathrm{d}m + a_{31}\,\mathrm{d}\omega + a_{32}\,\mathrm{d}\varphi + a_{33}\,\mathrm{d}\kappa \end{aligned} \tag{6}$$

where a_{ij} are the coefficient terms whose expansions are trivial.

Using the following notation

$$g_x = \frac{\partial g^0(x,y,z)}{\partial x}, \quad g_y = \frac{\partial g^0(x,y,z)}{\partial y}, \quad g_z = \frac{\partial g^0(x,y,z)}{\partial z} \tag{7}$$

and substituting Equations (6), Equation (4) results in the following:

$$
\begin{aligned}
-e(x,y,z) &= g_x\,\mathrm{d}t_x + g_y\,\mathrm{d}t_y + g_z\,\mathrm{d}t_z \\
&+ (g_x a_{10} + g_y a_{20} + g_z a_{30})\,\mathrm{d}m \\
&+ (g_x a_{11} + g_y a_{21} + g_z a_{31})\,\mathrm{d}\omega \\
&+ (g_x a_{12} + g_y a_{22} + g_z a_{32})\,\mathrm{d}\varphi \\
&+ (g_x a_{13} + g_y a_{23} + g_z a_{33})\,\mathrm{d}\kappa \\
&- (f(x,y,z) - g^0(x,y,z))
\end{aligned} \tag{8}
$$

In the context of the Gauss-Markoff model, each observation is related to a linear combination of the parameters, which are variables of a deterministic unknown function. The terms $\{g_x, g_y, g_z\}$ are numeric first derivatives of this function $g(x, y, z)$.

Equation (8) gives in matrix notation

$$
-\boldsymbol{e} = \mathbf{A}\boldsymbol{x} - \boldsymbol{l} \quad , \quad \mathbf{P} \tag{9}
$$

where $\mathbf{A}$ is the design matrix, $\mathbf{P} = \mathbf{P}_{ll}$ is the a priori weight matrix, $\boldsymbol{x}^{\mathrm{T}} = [\mathrm{d}t_x\ \mathrm{d}t_y\ \mathrm{d}t_z\ \mathrm{d}m\ \mathrm{d}\omega\ \mathrm{d}\varphi\ \mathrm{d}\kappa]$ is the parameter vector, and $\boldsymbol{l} = f(x, y, z) - g^0(x, y, z)$ is the discrepancy vector that consists of the Euclidean distances between the template and correspondent search surface elements. In our implementation, the template surface elements are approximated by the data points. On the other hand, the search surface elements are represented by user selection of one of the two different type of piecewise surface forms (planar and bi-linear). In general, both surfaces can be represented in any kind of piecewise form.

With the statistical expectation operator $\mathrm{E}\{\}$ and the assumptions

$$
\boldsymbol{e} \sim \mathrm{N}(0, \sigma_0^2 \mathbf{Q}_{ll}) \quad , \quad \sigma_0^2 \mathbf{Q}_{ll} = \sigma_0^2 \mathbf{P}_{ll}^{-1} = \mathbf{K}_{ll} = \mathrm{E}\{\boldsymbol{e}\boldsymbol{e}^{\mathrm{T}}\} \tag{10}
$$

the system (9) and (10) is a Gauss-Markoff estimation model. $\mathbf{Q}_{ll}$ and $\mathbf{K}_{ll}$ stand for a priori cofactor and covariance matrices, respectively.

The unknown transformation parameters are treated as stochastic quantities using proper a priori weights. This extension gives advantages of control over the estimating parameters. We introduce the additional observation equations for the system parameters as

$$
-\boldsymbol{e}_b = \mathbf{I}\boldsymbol{x} - \boldsymbol{l}_b \quad , \quad \mathbf{P}_b \tag{11}
$$

where $\mathbf{I}$ is the identity matrix, $\boldsymbol{l}_b$ is the (fictitious) observation vector for the system parameters, and $\mathbf{P}_b$ is the associated weight coefficient matrix. The weight matrix $\mathbf{P}_b$ has to be chosen appropriately, considering a priori information of the parameters. An infinite weight value ($(\mathbf{P}_b)_{ii} \to \infty$) excludes the i-th parameter from the system assigning it as constant, whereas zero weight ($(\mathbf{P}_b)_{ii} = 0$) allows the i-th parameter to vary freely assigning it as free parameter in the classical meaning.

The Least Squares solution of the joint system Equations (9) and (11) gives as the Generalized Gauss-Markoff model the unbiased minimum variance estimation for the parameters

$$
\hat{\boldsymbol{x}} = (\mathbf{A}^{\mathrm{T}}\mathbf{P}\mathbf{A} + \mathbf{P}_b)^{-1}(\mathbf{A}^{\mathrm{T}}\mathbf{P}\boldsymbol{l} + \mathbf{P}_b\boldsymbol{l}_b) \qquad \text{solution vector} \tag{12}
$$

$$
\hat{\sigma}_0^2 = (\boldsymbol{v}^{\mathrm{T}}\mathbf{P}\boldsymbol{v} + \boldsymbol{v}_b^{\mathrm{T}}\mathbf{P}_b\boldsymbol{v}_b)/r \qquad \text{variance factor} \tag{13}
$$

$$
\boldsymbol{v} = \mathbf{A}\hat{\boldsymbol{x}} - \boldsymbol{l} \qquad \text{residual vector for surface observations} \tag{14}
$$

$$
\boldsymbol{v}_b = \mathbf{I}\hat{\boldsymbol{x}} - \boldsymbol{l}_b \qquad \text{residual vector for parameter observations} \tag{15}
$$

where ^ stands for the Least Squares Estimator, and r is the redundancy. Since the functional model is non-linear, the solution is obtained iteratively. In the first iteration the initial approximations of the parameters must be provided. After the solution vector (Equation 12) is solved, the search surface $g^0(x, y, z)$ is transformed to a new state using the updated set of transformation parameters, and the design matrix $\mathbf{A}$ and the discrepancies vector $\boldsymbol{l}$ are re-evaluated. The iteration stops if each element of the alteration vector $\hat{\boldsymbol{x}}$ in Equation (12) falls below a certain limit: $|\mathrm{d}p_i| < c_i$.

The numerical derivative terms $\{g_x, g_y, g_z\}$ are defined as local surface normals $\boldsymbol{n}$. Their calculation depends on the analytical representation of the search surface elements. The derivative terms are given as x-y-z components of the local normal vectors: $[g_x\ g_y\ g_z]^{\mathrm{T}} = \boldsymbol{n} = [n_x\ n_y\ n_z]^{\mathrm{T}}$.

The surface representation is carried out in two different forms optionally: a TIN form, which gives planar surface elements, and a grid mesh form, which gives bi-linear surface elements. Both of these are first degree C^0 continuous surface representations. Surface topology is established simply by reading the standard range scanner output files in ASCII format and loading them in the scan-line order. For the pointclouds which have an irregular or unconventional sampling principle (or pattern), a more complex surface mesh generation algorithm can be utilized. For the details we refer to Gruen and Akca (2005).

2.2 Error detection and execution aspects

The standard deviations of the estimated transformation parameters and the correlations between themselves may give useful information concerning the stability of the system and quality of the data content (Gruen, 1985):

$$
\hat{\sigma}_p = \hat{\sigma}_0 \sqrt{q_{pp}} \quad , \quad q_{pp} \in \mathbf{Q}_{xx} = (\mathbf{A}^{\mathrm{T}}\mathbf{P}\mathbf{A} + \mathbf{P}_b)^{-1} \tag{16}
$$

where $\mathbf{Q}_{xx}$ is the cofactor matrix for the estimated parameters.

Detection of false correspondences with respect to the outliers and occlusions is a crucial part of every surface matching method. We use the following strategies in order to localize and eliminate the outliers and the occluded parts.

A median type of filtering is applied prior to the matching. For each point, the distances between the central point and its k-neighborhood points are calculated. In our implementation, k is selected as 8. If most of those k-distance values are much greater than the average point density, the central point is likely to be an erroneous point on a poorly reflecting surface (e.g. window or glass) or a range artifact due to surface discontinuity (e.g. points on the object silhouette). The central point is discarded according to the number of distances, which are greater than a given distance threshold.

In the course of iterations a simple weighting scheme adapted from Robust Estimation Methods is used:

$$(\mathbf{P})_{ii} = \begin{cases} 1 & \text{if} \quad |(\boldsymbol{v})_i| < K\hat{\sigma}_0 \\ 0 & \text{else} \end{cases} \tag{17}$$

In our experiments K is selected as >10, since it is aimed to suppress only the large outliers. It can be changed according to a desired confidence level. Because of the high redundancy of a typical data set, a certain amount of occlusions and/or smaller outliers do not have significant effect on the estimated parameters. As a comprehensive strategy, Baarda's (1968) data-snooping method can be favorably used to localize the occluded or gross erroneous measurements.

Finally, the correspondences coinciding to mesh boundaries are excluded from the estimation. The mesh boundaries represent the model borders, additionally the data holes inside the model. The data holes are possibly due to occlusions. Rejecting the correspondences on the mesh boundaries effectively eliminates the occlusions.

The convergence behaviour of the proposed method basically depends on the quality of the initial approximations and quality of the data content. For a good data configuration case it usually achieves the solution after 5 or 6 iterations.

3. ACCELERATION STRATEGIES

3.1 Fast correspondence computation with boxing structure

The computational effort increases with the number of points in the matching process. The main portion of the computational complexity is to search the corresponding elements of the template surface on the search surface, whereas the parameter estimation part is a small system, and can quickly be solved using Cholesky decomposition followed by back-substitution. Searching the correspondence is guided by an efficient boxing structure (Chetverikov, 1991), which partitions the search space into cuboids. For a given surface element, the correspondence is searched only in the box containing this element and in the adjacent boxes. In the original publication (Chetverikov, 1991) it was given for 2D point sets. We straightforwardly extend it to the 3D case. For the implementation details we refer to (Akca and Gruen, 2005b). The access procedure requires O(q) operations, where q is the average number of points in the box. It is easy to implement and time-effective for accessing the data.

In our implementation, the correspondence is searched in the boxing structure during the first few iterations, and in the meantime its evolution is tracked across the iterations. Afterwards the searching process is carried out only in an adaptive local neighborhood according to the previous position and change of correspondence. In any step of the iteration, if the change of correspondence for a surface element exceeds a limit value, or oscillates, the search procedure for this element is returned to the boxing structure again.

3.2 Simultaneous multi-subpatch matching

The basic estimation model can be implemented in a multi-patch mode, that is the simultaneous matching of two or more search surfaces $g_i(x, y, z)$, $i = 1,\ldots, k$ to one template $f(x, y, z)$.

$$\begin{aligned} -\boldsymbol{e}_1 &= \mathbf{A}_1 \boldsymbol{x}_1 - \boldsymbol{l}_1 \quad , \ \mathbf{P}_1 \\ -\boldsymbol{e}_2 &= \mathbf{A}_2 \boldsymbol{x}_2 - \boldsymbol{l}_2 \quad , \ \mathbf{P}_2 \\ &\vdots \qquad\qquad \vdots \\ -\boldsymbol{e}_k &= \mathbf{A}_k \boldsymbol{x}_k - \boldsymbol{l}_k \quad , \ \mathbf{P}_k \end{aligned} \tag{18}$$

Since the parameter vectors $\boldsymbol{x}_1, \ldots, \boldsymbol{x}_k$ do not have any joint components, the sub-systems of Equation (18) are orthogonal to each other. In the presence of auxiliary information, those sets of equations could be connected via functional constraints, e.g. as in the geometrically constrained multiphoto matching (Gruen, 1985; Gruen and Baltsavias, 1988) or via appropriate formulation of multiple (>2) overlap conditions.

An ordinary pointcloud includes enormously redundant information. A straightforward way to register such two pointclouds could be matching of the whole overlapping areas. This is computationally expensive. We propose multi-subpatch mode as a further extension to the basic model, which is capable of simultaneous matching of sub-surface patches, which are interactively selected in cooperative surface areas. They are joined to the system by the same 3D transformation parameters. This leads to the observation equations

$$\begin{aligned} -\boldsymbol{e}_1 &= \mathbf{A}_1 \boldsymbol{x} - \boldsymbol{l}_1 \quad , \ \mathbf{P}_1 \\ -\boldsymbol{e}_2 &= \mathbf{A}_2 \boldsymbol{x} - \boldsymbol{l}_2 \quad , \ \mathbf{P}_2 \\ &\vdots \qquad\qquad \vdots \\ -\boldsymbol{e}_k &= \mathbf{A}_k \boldsymbol{x} - \boldsymbol{l}_k \quad , \ \mathbf{P}_k \end{aligned} \tag{19}$$

with $i = 1,\ldots, k$ subpatches. They can be combined as in Equation (9), since the common parameter vector $\boldsymbol{x}$ joints them to each other. The individual subpatches may not include sufficient information for the matching of whole surfaces, but together they provide a computationally effective solution, since they consist of only relevant information rather than using the full data set.

4. EXPERIMENTAL RESULTS

Two practical examples are given to show the capabilities of the method. All experiments were carried out using own self-developed C/C++ software that runs on an Intel® P4 2.53Ghz PC. In all experiments the initial approximations of the unknowns were provided by interactively selecting 3 common points on both surfaces before matching. The scale factor m was fixed to unity by infinite weight value ($(\mathbf{P}_b)_{ii} \rightarrow \infty$).

The first example is the registration of two point clouds of a newspaper page (Fig. 1). The scanning was performed by using the stereoSCAN^{3D} system developed by Breuckmann GmbH (Germany). It is a high accurate scanner system based on the fringe projection technique.

The average point spacing is 150 ~ 170 microns. The surface of Figure 1a was matched to the one in Figure 1b by use of the LS3D surface matching. The iteration criteria values c_i were selected as 1 micron for the translation vector and 10^{cc} for the rotation angles. Although it is a difficult example due to very little changes in surface curvature, the matching is successful (Fig. 1c). Totally 377,234 points were used for matching. The a posteriori sigma value was 11.3 microns, with 13 iterations in 36.7 seconds. Interestingly, the letters are clearly visible on the surface model (Fig. 1c). However, they are due to range artifacts created by the pixel-discretization on the chip level, leading to intensity discontinuities. For a detailed discussion of the range artifacts we refer to Blais et al. (2005).

A comparison against the non-accelerated version was made. The non-accelerated version exhaustively searches the correspondence in a large portion of the search surface during the first few iterations. In the following iterations it uses the same adaptive local neighborhood search as in the accelerated version. For a fair comparison same number of points were employed in the matching. The non-accelerated version found the same solution in 106.1 seconds. As seen in this experiment, the accelerated version speeds the computation up typically by factor 2 to 3 (Akca and Gruen, 2005b). This is the sole effect of the space partitioning technique.

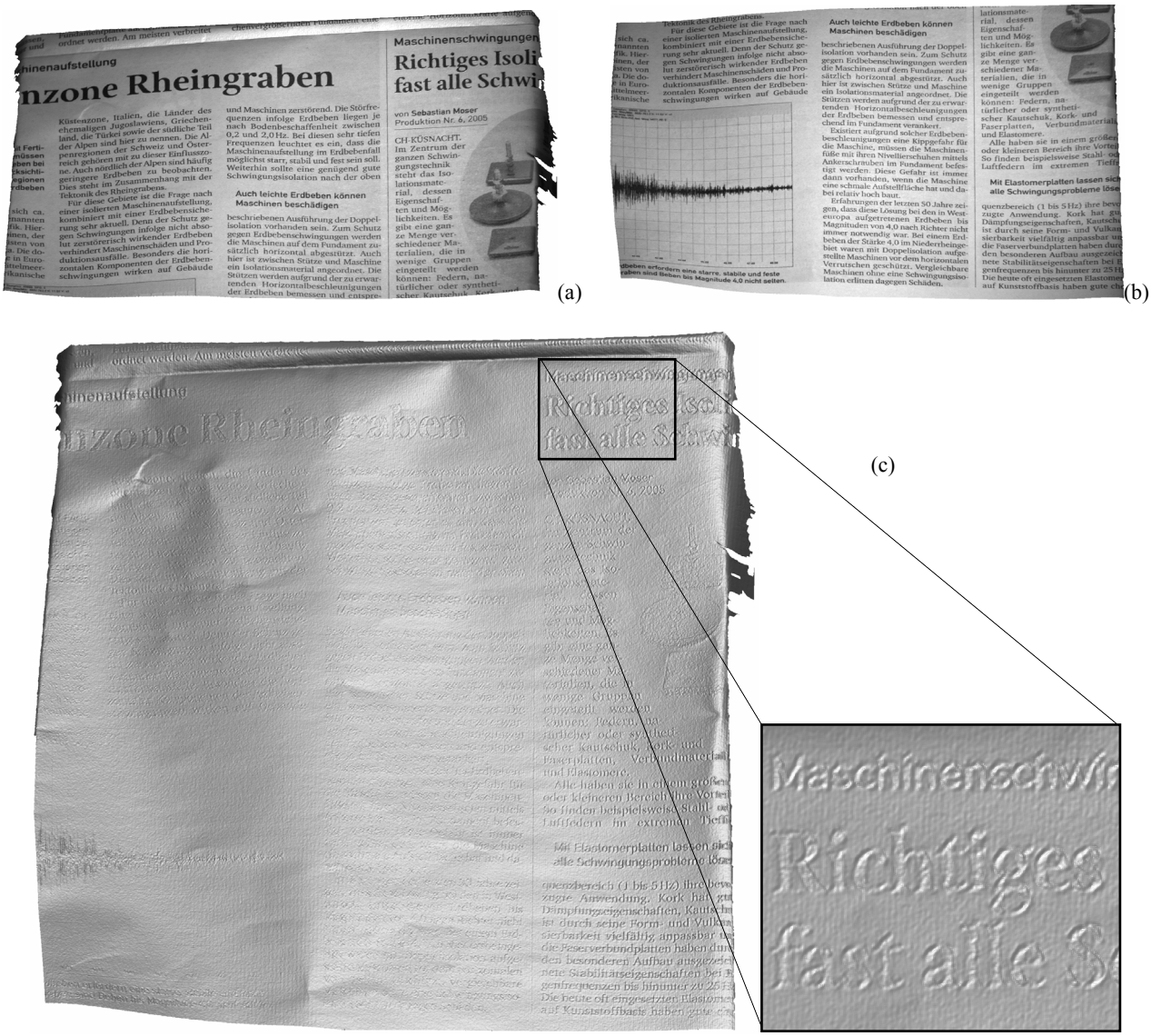

Figure 1: Example "newspaper". (a) Search and (b) template surfaces, (c) shaded view of the final composite surface after the LS3D surface matching. Zoom-in part of (c) shows the range artifacts due to intensity discontinuities. Note that the scanner derived intensities are back-projected onto the surfaces (a) and (b) only for the visualization purposes, they are not used in matching.

The second experiment refers to the matching of point clouds of a wooden Buddha statue (ca 30x40x20 cm^3). It has a very shiny polished surface (Fig. 2a), which is not an optimal surface reflectivity case. In a recent study Remondino et al. (2005) have modeled the same object using the photogrammetric technique and additionally the BIRIS laser scanner. In our experiment the point clouds were acquired by the triTOS system, which is another structured light-based scanner product of Breuckmann GmbH. It is mainly used for art and cultural heritage applications.

The data set contains 15 scans, each of which has ca 1.4 million points. The average point spacing is 0.3 ~ 0.5 millimeters. Nineteen consecutive matching processes were performed using the simultaneous multi-subpatch approach of the LS3D matching method. The iteration criteria values c_i were selected as 0.1 micron for the translation vector and 10^{cc} for the rotation angles. The average numerical results of the matching are given in Table 1.

The first scan was selected as the reference, which defines the datum of the common coordinate system. Since it is a closed object, there is need for a global registration, which distributes the residuals evenly among all the scans, and also considers the closure condition, i.e. matching of the last scan to the first one. For this purpose we used the block adjustment by independent model solution, which was formerly proposed for global

registration of laser scanner point clouds, but for the case of retro-reflective targets as tie points (Scaioni and Forlani, 2003). In the LS3D matching processes, the final correspondences were saved to separate files. Then all these files were given as input to a block adjustment by an independent model procedure, which concluded with 42 microns a posteriori sigma value. At this step the model contains ca. 9.5 million triangles. Using Geomagic Studio v.6 (Raindrop Geomagic) all surfaces were merged as one manifold, in parallel reducing the number of triangles to ca. 3 million and applying a low level noise reduction (Fig. 2b).

Figure 2: Example "wooden Buddha". (a) The wooden Buddha statue, (b) shaded view of the generated 3D model.

Table 1: The matching (use of subpatch technique) results of the "wooden Buddha" example.

Average no. of employed points	Average no. of iterations	Average CPU times (sec.)	Average *a posteriori* sigma values (micron)
100 ~ 400K	4 ~ 11	9 ~ 52	66 ~ 105

5. CONCLUSIONS

An algorithm for the least squares matching of overlapping 3D surfaces is presented. Our proposed method, the Least Squares 3D surface matching (LS3D), estimates the transformation parameters of one or more fully 3D surfaces with respect to a template one, using the Generalized Gauss Markoff model, minimizing the sum of squares of the Euclidean distances between the surfaces. The mathematical model is a generalization of the least squares image matching method and offers high flexibility for any kind of 3D surface correspondence problem. The least squares concept allows for the monitoring of the quality of the final results by means of precision and reliability criterions.

The practical example shows that our proposed method can provide successful matching results in reasonable processing times. The use of our space partitioning technique alone leads to a speed up of computing times by factor 2-3. Another aspect of our experiment is that registration task can be performed automatically without using retro-reflective or other special kinds of targets even for the surfaces with little geometric information.

6. REFERENCES

Akca, D., Gruen, A., 2005a. A flexible mathematical model for matching of 3D surfaces and attributes. Videometrics VIII, Proc. of SPIE-IS&T Electronic Imaging, San Jose (California), USA, January 18-20, SPIE vol. 5665, pp.184-195.

Akca, D., Gruen, A., 2005b. Fast correspondence search for 3D surface matching. ISPRS Workshop Laser scanning 2005, Enschede, the Netherlands, September 12-14. International Archives of the Photogrammetry, Remote Sensing and Spatial Information Sciences, vol. XXXVI, part 3/W19, pp. 186-191.

Arun, K.S., Huang, T.S., and Blostein, S.D., 1987. Least-squares fitting of two 3D point sets. IEEE Transactions on Pattern Analysis and Machine Intelligence 9 (5), 698-700.

Baarda, W., 1968. A testing procedure for use in geodetic networks. Netherlands Geodetic Commission, Delft, Vol. 2, No. 5, 97 p.

Bergevin, R., Soucy, M., Gagnon, H., and Laurendeau, D., 1996. Towards a general multi-view registration technique. IEEE PAMI, 18(5), 540-547.

Besl, P.J., and McKay, N.D., 1992. A method for registration of 3D shapes. IEEE PAMI, 14(2), 239-256.

Blais, G., and Levine, M.D., 1995. Registering multiview range data to create 3D computer objects. IEEE PAMI, 17(8), 820-824.

Blais, F., Taylor, J., et al., 2005. Ultra-high resolution imaging at 50 µm using a portable XYZ-RGB color laser scanner. Int. Workshop on Recording, Modeling and Visualization of Cultural Heritage, Ascona, May 22-27.

Campbell, R.J., and Flynn, P.J., 2001. A survey of free-form object representation and recognition techniques. CVIU, 81(2), 166-210.

Chen, Y., and Medioni, G., 1992. Object modelling by registration of multiple range images. IVC, 10(3), 145-155.

Chetverikov, D., 1991. Fast neighborhood search in planar point sets. Pattern Recognition Letters, 12(7), 409-412.

Chetverikov, D., Stepanov, D., and Krsek, P., 2005. Robust Euclidean alignment of 3D point sets: the trimmed iterative closest point algorithm. IVC, 23(3), 299-309.

Dalley, G., and Flynn, P., 2002. Pair-wise range image registration: a case study in outlier classification. CVIU, 87(1-3), 104-115.

Dorai, C., Weng, J., and Jain, A.K., 1997. Optimal registration of object views using range data. IEEE PAMI, 19(10), 1131-1138.

Ebner, H., and Strunz, G., 1988. Combined point determination using Digital Terrain Models as control information. IAPRS, 27(B11/3), 578-587.

Eggert, D.W., Lorusso, A., and Fisher, R.B., 1997. Estimating 3D rigid body transformations: a comparison of four major algorithms. MVA, 9(5-6), 272-290.

Faugeras, O.D., and Hebert, M., 1986. The representation, recognition, and locating of 3-D objects. The International Journal of Robotics Research 5 (3), 27-52.

Feldmar, J., and Ayache, N., 1996. Rigid, affine and locally affine registration of free-from surfaces. International Journal of Computer Vision 18 (2), 99-119.

Fitzgibbon, A.W., 2001. Robust registration of 2D and 3D point sets. British Machine Vision Conference, Manchester, September 10-13, pp. 411-420.

Gruen, A., 1985. Adaptive least squares correlation: a powerful image matching technique. South Afr. J. of Photog., Remote Sensing and Cartography, 14(3), 175-187.

Gruen, A., Baltsavias, E.P., 1988. Geometrically constrained multiphoto matching. PE & RS, 54(5), 633-641.

Gruen, A., and Akca, D., 2005. Least squares 3D surface and curve matching. ISPRS J. of Photogrammetry & Remote Sensing, 59(3), 151-174.

Guehring, J., 2001. Reliable 3D surface acquisition, registration and validation using statistical error models. IEEE 3DIM'01, Quebec, May 28-June 1, pp. 224-231.

Horn, B.K.P., 1987. Closed-form solution of absolute orientation using unit quaternions. Journal of the Optical Society of America A-4 (4), 629-642.

Horn, B.K.P., Hilden, H.M., and Negahdaripour, S., 1988. Closed-form solution of absolute orientation using orthonormal matrices. Journal of the Optical Society of America A-5 (7), 1128-1135.

Jokinen, O., and Haggren, H., 1998. Statistical analysis of two 3-D registration and modeling strategies. ISPRS J. of Photogrammetry & Remote Sensing, 53(6), 320-341.

Jost, T., and Huegli, H., 2003. A multi-resolution ICP with heuristic closest point search for fast and robust 3D registration of range images. IEEE 3DIM'03, Banff, pp. 427-433.

Maas, H.G., 2000. Least-Squares Matching with airborne laserscanning data in a TIN structure. IAPRS, 33(3A), 548-555.

Masuda, T., and Yokoya, N., 1995. A robust method for registration and segmentation of multiple range images. CVIU, 61(3), 295-307.

Neugebauer, P.J., 1997. Reconstruction of real-world objects via simultaneous registration and robust combination of multiple range images. IJSM, 3(1-2), 71-90.

Okatani, I.S., and Deguchi, K., 2002. A method for fine registration of multiple view range images considering the measurement error properties. CVIU, 87(1-3), 66-77.

Pajdla, T., and Van Gool, L., 1995. Matching of 3-D curves using semi-differential invariants. IEEE ICCV'95, Cambridge (MA), June 20-23, pp. 390-395.

Park, S.Y., and Subbarao, M., 2003. A fast point-to-tangent plane technique for multi-view registration. IEEE 3DIM'03, Banff, October 6-10, pp. 276-283.

Postolov, Y., Krupnik, A., and McIntosh, K., 1999. Registration of airborne laser data to surfaces generated by Photogrammetric means. IAPRS, 32(3/W14), 95-99.

Potmesil, M., 1983. Generating models of solid objects by matching 3D surface segments. International Joint Conference on Artificial Intelligence, Karlsruhe, August 8-12, pp. 1089-1093.

Pulli, K., 1999. Multiview registration for large data sets. IEEE 3DIM'99, Ottawa, October 4-8, pp. 160-168.

Remondino, F., Guarnieri, A., and Vettore, A., 2005. 3D modeling of close-range objects: photogrammetry or laser scanning? Videometrics VIII, San Jose, pp.216-225.

Rosenholm, D., and Torlegard, K., 1988. Three-dimensional absolute orientation of stereo models using Digital Elevation Models. PE & RS, 54(10), 1385-1389.

Rusinkiewicz, S., and Levoy, M., 2001. Efficient variants of the ICP algorithm. IEEE 3DIM'01, Quebec, May 28–June 1, pp. 145-152.

Scaioni, M., and Forlani, G., 2003. Independent model triangulation of terrestrial laser scanner data. IAPRS, 34(5/W12), 308-313.

Schenk, T., Krupnik, A., and Postolov, Y., 2000. Comparative study of surface matching algorithms. IAPRS, 33(B4), 518-524.

Szeliski, R., and Lavallee, S., 1996. Matching 3-D anatomical surfaces with non-rigid deformations using octree-splines. Int. Journal of Computer Vision, 18(2), 171-186.

Turk, G., and Levoy, M., 1994. Zippered polygon meshes from range images. ACM SIGGRAPH'94, Orlando (Florida), July 24-29, pp. 311-318.

Williams, J.A., Bennamoun, M., Latham, S., 1999. Multiple view 3D registration: A review and a new technique. IEEE SMC'99, Tokyo, October 12-15, pp. 497-502.

Zhang, Z., 1994. Iterative point matching for registration of free-form curves and surfaces. Int. Journal of Computer Vision, 13(2), 119-152.